Pumped Thermal Electricity Storage with Supercritical CO_2 Cycles and Solar Heat Input

Joshua McTigue [1, a)] Pau Farres-Antunez [2, b)], Kevin Ellingwood [3, c)], Ty Neises [1, d)], and Alexander White [2, e)]

[1] *National Renewable Energy Laboratory, 15013 Denver West Parkway, Golden, CO, 80401, USA*
[2] *Cambridge University Engineering Department, Trumpington Street, Cambridge, CB2 1PZ, UK*
[3] *University of Utah, 201 Presidents Cir, Salt Lake City, UT, 84112, USA*

[a)] Corresponding author: JoshuaDominic.McTigue@nrel.gov
[b)] pf298@cam.ac.uk
[c)] k.ellingwood@utah.edu
[d)] Ty.Neises@nrel.gov
[e)] ajw36@cam.ac.uk

Abstract. Pumped Thermal Electricity Storage (PTES) is an energy storage device that uses grid electricity to drive a heat pump that generates hot and cold storage reservoirs. This thermal potential is later used to power a heat engine and return electricity to the grid. In this article, a PTES variant that uses supercritical carbon dioxide (sCO_2) as the working fluid is introduced. sCO_2-PTES cycles have higher work ratios and power densities than the systems based on ideal gases that have been investigated to date. Furthermore, sCO_2-PTES cycles may achieve higher round-trip efficiencies for a given hot storage temperature (up to 78% at 560°C). The sensitivity of PTES cycles to loss factors such as isentropic efficiencies and temperature differences between the power cycle and storage fluid is investigated. A second concept whereby an sCO_2-PTES cycle is integrated with concentrating solar power (CSP) is introduced. This concept 'time-shifts' the recompression of an sCO_2 recompression cycle to a period of lower electricity prices and stores the heat. When solar heat is dispatched, the recompressor may be avoided as the required heat is obtained from storage, thereby leading to increased heat engine efficiencies. The net work output of this integrated system is 10-18% greater than the conventional recompression cycle. Combining PTES with a CSP power cycle is therefore shown to improve the dispatch of solar heat as well as providing electricity storage services.

INTRODUCTION

Pumped Thermal Electricity Storage (PTES) is a grid-scale energy management device that stores electricity in a thermal potential between hot and cold media. PTES has been investigated globally under a variety of names and is being commercially developed. PTES has several advantages compared to other electricity storage devices, including no geographical restrictions, long lifetimes, and the ability to use cheap, abundant, non-toxic materials as the storage media. Furthermore, PTES can achieve reasonable round-trip efficiencies (up to 70%) and energy and power densities at competitive costs, as indicated in Table 1.

A number of PTES systems have been proposed based on different thermodynamic cycles, including Joule-Brayton cycles with ideal gases [1], without or with recuperation [2], transcritical CO_2 cycles [3], and cryogenic cycles [4]. Commercialization has so far concentrated on Joule-Brayton cycles with early concepts developed by SAIPEM [5] and Isentropic Ltd. [6]. Currently, Malta Inc. are developing a 10 MW_e / 80 MWh_e system based on the recuperated Joule-Brayton cycle with molten salts as storage media [7].

As a bulk electricity storage device, PTES may enable high penetrations of variable renewable generation on the electrical grid. Furthermore, because PTES relies on thermal energy storage it can potentially integrate with other systems that involve the transfer or exploitation of thermal energy. In particular, some versions of PTES share

important similarities with concentrating solar power (CSP) in terms of storage materials and temperature ranges employed, which facilitates the design of integrated systems.

Some researchers consider supercritical-carbon dioxide (sCO_2) cycles to be the next generation of power cycle for CSP. These cycles have the advantage of high efficiency, compact (potentially low-cost) machinery, and compatibility with dry-cooling technology. In this article, PTES concepts based on sCO_2 cycles are described. Results from Joule-Brayton cycles are also provided as a benchmark for performance. Two applications are discussed. Firstly, stand-alone PTES based on sCO_2 power cycles are introduced. These cycles can achieve high work ratios due to the real-gas properties of CO_2 close to the critical point, which leads to high efficiencies and low susceptibility to machinery losses. Secondly, a method to enhance a CSP cycle with a PTES system is introduced: in this concept an sCO_2 recompression cycle is combined with a heat pump and a thermal storage system. sCO_2 recompression cycles are highly recuperated and require that some flow is diverted through a 'recompressor' which operates at higher temperatures than the main pump. The recompressor can account for around 40% of the total work input to the power cycle. The recompression step may be 'time-shifted' to occur when electricity prices are lower and the heat of compression is stored in a hot storage medium. Later, when solar energy is dispatched through the sCO_2 power cycle, the recompressor is not required and heat is obtained from the hot storage instead.

In the next section, PTES concepts are discussed in more detail. sCO_2 PTES systems are then introduced, and their performance compared to ideal-gas PTES devices. Finally, the integration of PTES with CSP cycles is discussed and results are presented.

TABLE 1. Comparison of prominent electricity storage systems. PTES: Pumped Thermal Electricity Storage; PHS: Pumped Hydroelectric Storage; CAES: Compressed Air Energy Storage; Li-ion: Lithium-ion batteries. PTES offers GWh-scale storage without the geographic constraints suffered by PHS and CAES, at lower cost than battery technology. Data from Refs. [8–11]

		PTES	PHS	CAES	Li-ion
Round-trip efficiency	%	40 – 70	60 – 80	50 – 70	80 – 90
Energy density	kWh / m^3	50	1.4	10	250 – 750
Cost	$ / kWh	25 – 250	5 – 100	2 – 50	200 – 800
Cost	$ / kW	300 – 2800	600 – 2000	400 – 800	1000 – 1700

Nomenclature

Symbols

f_p	%	Pressure loss factor	P	Pa	Pressure
η_s	%	Isentropic efficiency	$\dot{q}$	J/kg	Specific heat
η_{rt}	%	Round-trip efficiency, see Eq. 1	ρ_P	W / (m^3/s)	Power density, see Eq. 2
$\eta_{rt,x}$	%	Exergetic round-trip efficiency, see Eq. 3	ρ_f	kg/m^3	Fluid density
η_{net}	%	Net efficiency, see Eq. 4	T	°C	Temperature
$\dot{m}$	kg/s	Mass flow rate	ΔT	°C	Temperature difference
			$\dot{w}$	J/kg	Specific work

Abbreviations

PTES	Pumped Thermal Electricity Storage
PHS	Pumped Hydro-electricity Storage
CAES	Compressed Air Energy Storage
Li-ion	Lithium-ion
sCO_2	Supercritical carbon dioxide
RC	Recompression
TSRC	Time-shifted recompression

Subscripts, superscripts

chg	Charge
dis	Discharge

PTES WORKING PRINCIPLE

PTES takes low-value power off the grid to create a temperature difference between two thermal reservoirs using a heat pump, and later exploits this temperature difference using a heat engine to produce electricity. A schematic of the charging cycle is shown in Figure 1. During charge, grid electricity is used to compress a fluid to high pressure and temperature, states 1→2. The hot fluid transfers its energy to a thermal storage media such as a packed bed of rocks or molten salt (2→3) before being expanded (and cooled) to its original pressure (3→4), before finally exchanging heat with the cold storage media (4→1). The charging process thus creates a cold store and a hot store. Energy is extracted during discharge by reversing the direction of the fluid flow. Cold fluid is compressed before heat is transferred from the hot store. The hot fluid is expanded to generate electricity and is finally cooled in the cold store.

The round-trip efficiency is defined as the net work output during discharge divided by the net work input during charge:

$$\eta_{rt} = \frac{\dot{W}_{\text{dis}}^{\text{net}}}{\dot{W}_{\text{chg}}^{\text{net}}} \tag{1}$$

If both the heat pump and heat engine achieve the Carnot limit, then the round-trip efficiency is 100%. In practice, irreversibilities caused by compression and expansion losses, pressure losses, and temperature differences between the power cycle and storage system reduce round-trip efficiencies to around 40-70%.

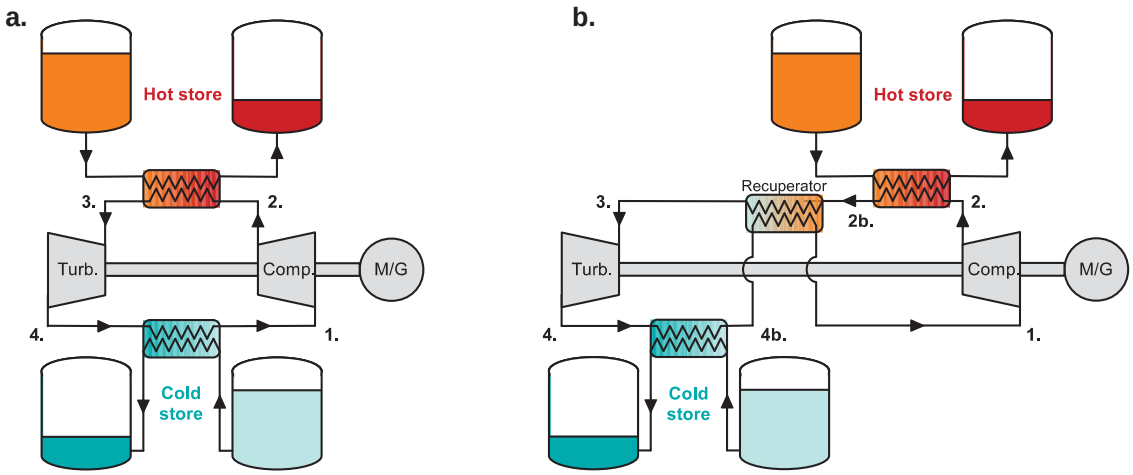

FIGURE 1: Schematic layout of PTES designs during charge. a) The concept used for sCO2 cycles b) A recuperated cycle with an ideal gas as the working fluid. Key: M/G – motor-generator; Turb. – turbine; Comp. – compressor.

PTES cycles typically require four turbomachines (two compressors and two turbines) and these components contribute significantly to the capital cost. The power density is a metric that indicates the power output of the cycle for a given size of turbomachinery, and is defined as:

$$\rho_P = \rho_{f,\text{min}} \dot{w}_{\text{dis}}^{\text{net}} \tag{2}$$

Where $\dot{w}_{\text{dis}}^{\text{net}}$ is the specific net work output in discharge and $\rho_{f,\text{min}}$ is the minimum fluid density around the cycle, which typically occurs at the discharging turbine exit. Cycles with higher density fluid (and therefore lower volumetric flows) will have more compact turbomachinery for a given power output, and this may lead to reduced power cycle costs.

Previous work has shown that cycle performance can be improved by maximizing the work ratio, which is the ratio of compression work to expansion work during charge [1,8]. Larger work ratios not only lead to higher round-trip efficiencies but also make the cycle less sensitive to losses in the turbomachinery. For an ideal gas, large work ratios can be obtained by (1) increasing the pressure ratio (or temperature ratio $T_2 \,/\, T_1$) (2) increasing T_1 (3) decreasing T_3. Using temperatures where T_1 is greater than T_3 facilitates the use of a recuperator, which is illustrated in Figure 1b. The recuperator reduces the operating temperature range of the storage material which facilitates the use of molten salts (which freeze below 200°C) for the hot storage system.

High work ratios can also be achieved by using real fluids such as supercritical CO_2 – operating part of the cycle close to the critical point increases the difference between the charging compression work and expansion work, see Figure 2. The critical pressure of CO_2 is 73.9 bar and operating the cycle above this pressure means that the high fluid densities will lead to high power densities. In this study, sCO_2 cycles are not recuperated as large variations in heat capacity between the high- and low-pressure fluid streams complicate the heat transfer processes.

SCO_2 CYCLES FOR PTES

Power cycle models have been developed that capture the dominant loss generating mechanisms. Isentropic efficiencies η_s are used for the compressors and expanders which are assumed to be rotating turbomachinery. Heat exchanger pressure losses are represented by a pressure loss factor, f_p, where $P_{\text{out}} = (1 - f_p)P_{\text{in}}$. Losses due to irreversible heat transfer in the heat exchangers are modelled by fixing a temperature difference ΔT between the fluids at each end of the exchanger. The objective of this work is to investigate the sensitivity of the proposed cycles to these loss factors. Subsequent work will refine these assumptions to more accurately assess the cycle performance.

PTES cycles based on supercritical CO_2 are primarily of interest here but recuperated ideal-gas PTES cycles using argon as the working fluid are also considered to provide a comparison. A nominal design is first developed for each power cycle, and design data is presented in Table 2. Nominal designs have isentropic efficiencies of 90%, pressure loss factors of 1% and heat exchanger temperature differences of 5°C. The nominal ideal-gas cycle is recuperated and uses argon as the working fluid, and the temperature-entropy diagram is shown in Figure 2. The maximum temperature T_2 is chosen to be 560°C which is compatible with nitrate molten salts. The charge compressor inlet temperature T_1 is effectively constrained by the recuperation process to be equal to the cold molten salt tank temperature, which is chosen to be 350°C to reduce the risk of the salt freezing. Together, this information fixes the charging compression ratio. The low-pressure side of this cycle is at 80 bar so that the system is comparable with the sCO_2 cycles (this value is substantially higher than those typically chosen for ideal-gas PTES which tends to be in the range of 1 bar [1] to 25 bar [4]). Cooling the gas to ambient temperatures (T_3 = 30°C) and then expanding through this pressure ratio creates a cold storage at $T_4 = -30.2$°C. The discharging pressure ratio is chosen such that the discharging expander outlet temperature is T_1 which ensures the recuperator operates between the same temperatures in charge and discharge. Under these conditions, the ideal-gas PTES cycle achieves a round-trip efficiency of 61.5%, see Table 2.

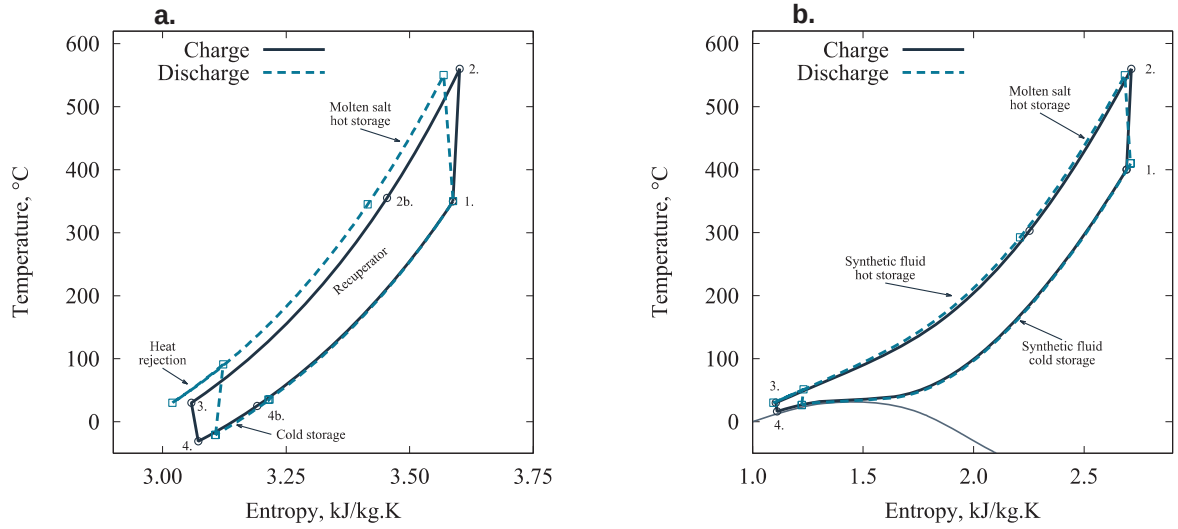

FIGURE 2. Temperature-entropy diagrams of PTES systems a) A recuperated ideal-gas Joule-Brayton cycle with argon as the working fluid. b) an sCO_2 power cycle with two fluids for the hot storage.

Two sCO_2 PTES nominal designs are considered: a high-temperature sCO_2 cycle with a maximum temperature of 560°C (see Figure 2b), and a low-temperature cycle with a maximum temperature of 200°C. The high-temperature cycle is comparable to the nominal ideal-gas cycle as both may use molten salts as the hot storage material. Both sCO_2 cycles have higher work ratios than the ideal-gas cycle. The low-temperature cycle has a comparable efficiency to the ideal-gas cycle at 60.4%, whereas the high-temperature sCO_2 cycle reaches $\eta_{rt} = 78.4\%$ because increasing T_2 leads

to both higher work ratios and round-trip efficiencies. To remain supercritical the sCO_2 cycles have a minimum pressure of 80 bar, and the maximum pressure is chosen to be in the range of 240-260 bar. The sCO_2 is more dense than argon, so that power densities are higher than the ideal-gas cycle. These values are very sensitive to the assumptions made about the loss factors η_s, f_p and ΔT and assuming $\Delta T = 5°C$ for cycles with supercritical fluids near the critical point may be unrealistically optimistic. The sensitivity to these loss factors is investigated in the next section but calculations of the heat exchanger performance are required to assess the true value of the loss factors.

While a higher sCO_2 temperature improves performance, it also complicates cycle design. For example, the sCO_2 cycle is not recuperated, and the hot storage must therefore operate between the maximum temperature and ambient temperature. As a result, the high-temperature cycle requires two sets of storage tanks: molten salts operate up to the maximum temperature, whilst a second fluid operates between ambient temperature and the molten salt freezing temperature. Synthetic fluids or mineral oils are suitable choices, although these fluids degrade over time, are relatively expensive, and require careful management of fire risk. For a given pressure ratio, the temperature of sCO_2 increases less than an ideal gas and charge compressor inlet temperatures T_1 are relatively high in comparison. As well as complicating the design of the charge compressor, the cold storage fluid therefore also operates over a wide temperature range. For the high-temperature sCO_2 cycle, the cold storage operates between 16°C and 400°C, requiring either a combination of storage fluids or the use of a synthetic fluid such as Biphenyl/Diphenyl Oxide.

The low-temperature sCO_2 PTES cycle potentially provides competitive performance with the ideal-gas cycle without the complications that come with higher temperatures. For instance, the hot and cold storage operate over smaller temperature ranges meaning that only one storage system is required for each of the hot and cold storage. Water can potentially be used as the cold storage material, which would reduce the cost and risk of using an alternative fluid. Lower temperatures provide less extreme operating conditions and could potentially simplify the design of turbomachinery, valves, seals and pipework and allow the use of more affordable materials.

The impact of loss factors on round-trip efficiency is investigated for isentropic efficiencies in the range of 75 - 100% and temperature differences between the storage fluid and power cycle between 0°C and 25°C. Unsurprisingly, increasing the loss factors reduces the PTES round-trip efficiency, as shown in Figure 3. The sCO_2 cycles are affected less significantly by the isentropic efficiency than the ideal-gas cycle, which is more sensitive to compression and expansion losses as a result of a lower work ratio [8]. Increasing the sCO_2 maximum temperature is also beneficial as this leads to higher work ratios and therefore lower sensitivity to the isentropic efficiency.

TABLE 2. Nominal designs for three PTES cycles. Parameters are varied about these nominal design points in the following studies.

		Ideal-gas cycle	Low temp. sCO_2	High temp. sCO_2
Working fluid		argon	CO_2	CO_2
T_1	°C	350.0	100.0	400.0
T_2	°C	560.0	200.0	560.0
T_3	°C	30.0	30.0	30.0
T_4	°C	-30.2	17.7	16.3
P_1	bar	80.0	80.0	80.0
β_{chg}		1.94	2.73	3.06
β_{dis}		2.20	2.44	3.26
Work ratio		3.91	5.22	10.9
Power density	kW / (m^3/s)	3.12	4.73	7.83
Round-trip efficiency	%	61.5	60.4	78.4
Isentropic efficiency	%	90.0		
Pressure loss factor	%	1.0		
ΔT	°C	5.0		

The temperature difference between the storage fluid and power cycle working fluid has a more significant effect on sCO_2 cycles than ideal-gas cycles. sCO_2 cycles transfer large quantities of heat per unit work input compared to ideal-gas cycles. For instance, the high-temperature sCO_2 cycle has a heat-to-work ratio $(|\dot{q}_{\mathrm{in}}| + |\dot{q}_{\mathrm{out}}|) / \dot{w}_{\mathrm{chg}}^{\mathrm{net}}$ of 8.8, which is 44% greater than that of the ideal-gas cycle (6.1) (see Refs. [10,12]). Therefore, any reduction in heat transfer effectiveness has a significant impact on cycle performance. The sCO_2 cycles show a particularly steep drop in performance at around $\Delta T = 10°C$, which corresponds to the point where discharging compression starts to occur at temperatures above the critical temperature, leading to a sudden decrease in net discharging work.

The impact of operational parameters (temperatures and pressures) is shown in Figure 4. For a fixed pressure ratio, the round-trip efficiency is improved by increasing the maximum cycle temperature T_2, with sCO_2 cycles achieving higher efficiencies than ideal-gas cycles for the assumed loss factors. However, the technological implications should be considered, as higher values of T_1 and T_2 may require more expensive materials. In Figure 4b, T_2 is held constant while the pressure ratio β (and therefore T_1) is varied. Larger pressure ratios lead to higher power densities, but optimum pressure ratios exist, which is similar to gas turbine behavior. These results are consistent with previous work on PTES cycles [1,8] but serve to illustrate that sCO_2-based PTES cycles also follow these trends, and potentially have better performance than ideal-gas cycles.

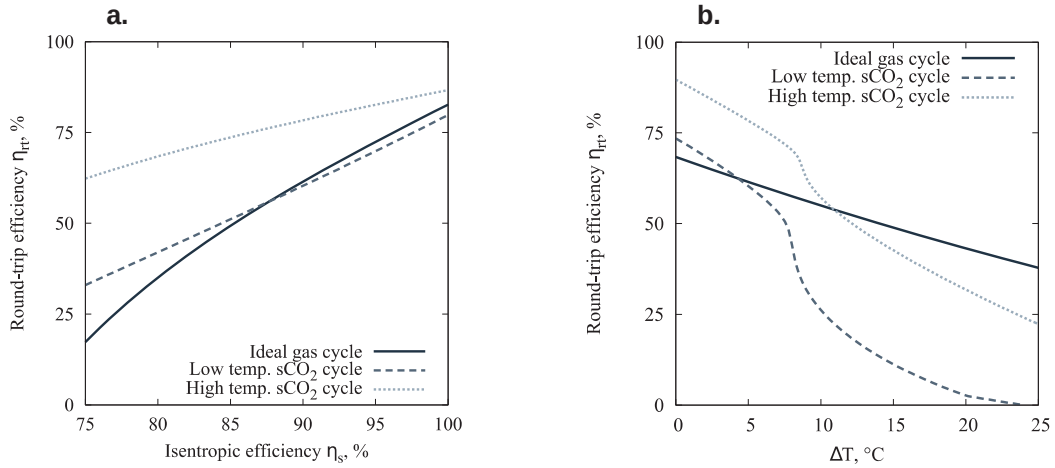

FIGURE 3. Effect of loss factors on PTES round-trip efficiency a) Isentropic efficiency is varied (all compressors and expanders have equal isentropic efficiency) b) The temperature difference ΔT between the power cycle and the storage fluid is varied

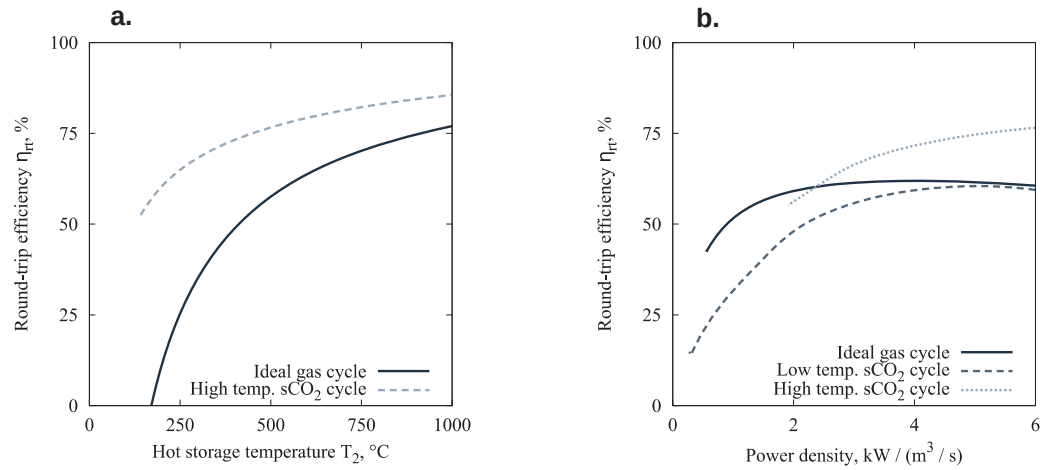

FIGURE 4. a) Variation of round-trip efficiency with maximum storage temperature. Pressure ratio is fixed while T_1 is increased. b) Variation of round-trip efficiency and power density. The maximum storage temperature is fixed, while the pressure ratio (and thus T_1) is varied.

sCO_2 POWER CYCLE WITH TIME-SHIFTED RECOMPRESSION

Supercritical-CO_2 power cycles are considered by some to be the next generation of power cycles for CSP due to high efficiencies, compact machinery and compatibility with dry-cooling [13]. These cycles are highly recuperated but large variations in real-gas heat capacities near the critical point leads to pinch point constraints. In the sCO_2 recompression (RC-sCO_2) cycle some flow is diverted into a higher-temperature compressor (the 'recompressor') which reduces the flow through the cold side of the low-temperature recuperator in order to match the fluid capacitance rates [14]. However, the recompressor pressurizes a higher temperature and lower density fluid than the main sCO_2 pump and accounts for around 40% of the total work input to the RC-sCO_2 cycle.

The net power output of an sCO_2 cycle can be increased by providing additional heat by means other than a recompressor. One option is to 'time-shift' the recompression to periods of low value electricity. The heat of compression is stored in a hot storage media. Later, when solar energy is dispatched through the sCO_2 power cycle, the recompressor is not required and heat is obtained from the hot storage instead. While the net electricity dispatched over a charge-discharge cycle is similar to the conventional recompression cycle, the specific power output that is dispatched at the most valuable times is increased.

If the time-shifted recompression forms the compression stage of a heat pump then a subsequent expansion can be used to create a cold store. A schematic of the charging cycle heat pump is shown in Figure 5, and is similar to conventional PTES cycles in Figure 1. The dispatch of solar energy then requires the discharge of the hot storage, as illustrated in Figure 6 and Figure 7. Furthermore, discharging the cold storage can reduce heat rejection temperature, thereby further reducing compression work and leading to a modest increase in heat engine efficiency. This cycle uses the same components as a conventional RC-sCO_2 cycle, and requires the addition of storage systems, a charging expander, and a small additional pump for discharge. Thus, an RC-sCO_2 cycle could hypothetically be retrofitted with the heat pump components, thereby creating a more flexible device.

Additional metrics are introduced here to evaluate the performance of the time-shifted sCO_2 recompression (TSRC-sCO_2) cycle. Comparing the electrical work input during charge to the electrical work output during discharge provides valuable information about the rate at which electricity can be stored and dispatched. However, using the conventional definition of round-trip efficiency (Eq. 1) leads to values greater than 100% due to the solar heat input. An *exergetic* round-trip efficiency may be defined by considering the maximum work that can be extracted from the solar heat input to the cycle. The exergetic round-trip efficiency $\eta_{rt,x}$ is given by:

$$\eta_{rt,x} = \frac{\dot{W}_{\text{dis}}^{\text{net}}}{\dot{W}_{\text{chg}}^{\text{net}} + \Delta\text{Ex}_{\text{solar}}} \tag{3}$$

Where $\Delta\text{Ex}_{\text{solar}} = \dot{m}\left(h_{in} - h_{out} - T_o(s_{in} - s_{out})\right)$ is the maximum work that could be extracted from the solar heat input.

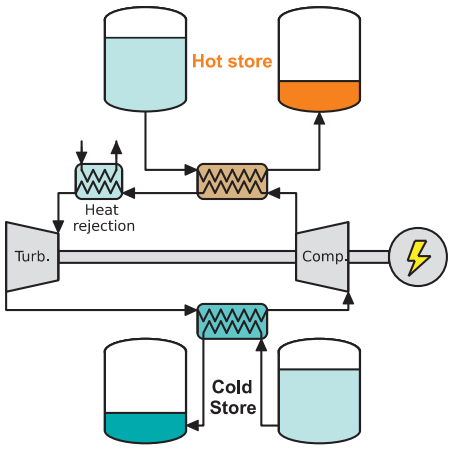

FIGURE 5. Schematic diagram of the heat pump charging phase that creates a hot storage to replace the recompressor in an sCO_2 cycle. A cold storage is also generated.

The TSRC-sCO$_2$ cycle uses grid electricity to charge the hot and cold storage. This electricity consumption should be considered when assessing the net electricity generation of the system. The TSRC-sCO$_2$ cycle can be compared to the conventional use of solar heat in a heat engine with the net efficiency, which is defined as

$$\eta_{\text{net}} = \frac{\dot{W}_{\text{dis}}^{\text{net}} - \dot{W}_{\text{chg}}^{\text{net}}}{\dot{Q}_{\text{solar}}} \tag{4}$$

Where $\dot{Q}_{\text{solar}}$ is the solar heat added to the system. The net efficiency effectively compares the storage system to a conventional solar heat engine under the assumption that the value of electricity is always constant. However, the TSRC-sCO$_2$ system may be able to take advantage of electricity price fluctuations as well as providing electricity storage services.

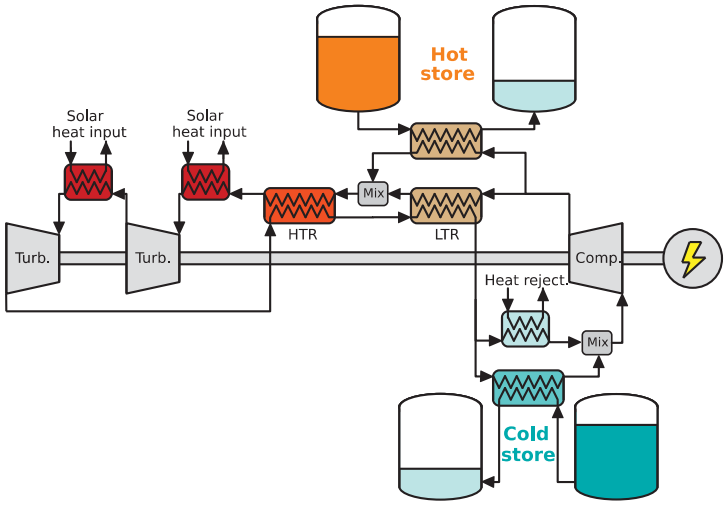

FIGURE 6. Schematic diagram of a time-shifted recompression sCO$_2$ cycle, where the recompression is replaced by heat from hot storage. Cold storage can also be used to reduce the compressor inlet temperature.

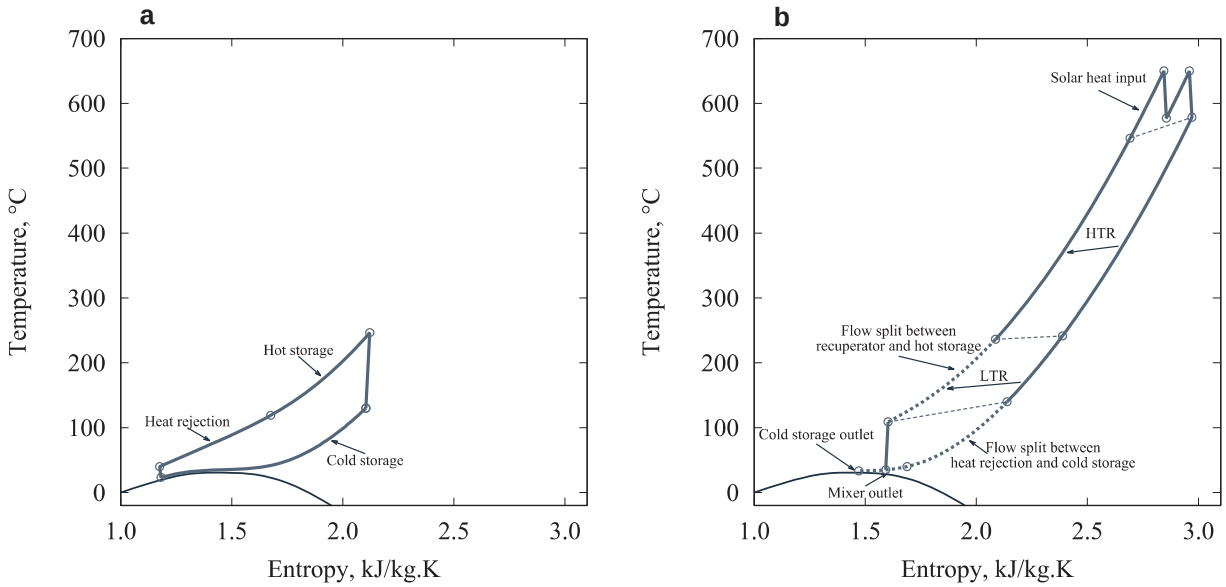

FIGURE 7. Temperature-entropy diagram of an sCO$_2$ cycle with time-shifted recompression a) Charging process b) Discharging process. Key: HTR – high temperature recuperator; LTR – low temperature recuperator

Nominal design data and performance of an sCO_2 recompression cycle is compared to the time-shifted recompression cycle in Table 3. Results are shown for TSRC-sCO_2 cycles with and without the cold storage being used to reduce heat rejection temperatures. These nominal designs have a turbine inlet temperature of 650°C, and the RC-sCO_2 cycle has a heat engine efficiency of 48.6%. TSRC-sCO_2 cycles achieve a 10% increase in discharging net work output with a heat engine efficiency of 53.8% as a result of reduced compressor work input during discharge. However, TSRC-sCO_2 cycle net efficiency is less than the RC-sCO_2 cycle heat engine efficiency as more flow is recompressed in the storage phase in order to overcome heat transfer losses between the power cycle and storage fluid.

The cold storage contains sufficient energy to cool the discharging compressor inlet temperature from 40°C to 35°C. This leads to a further increase in discharging work output and heat engine efficiency. The net efficiency is slightly lower than the time-shifted cycle without cold storage. Therefore, the additional cost of the cold storage and heat exchangers should be compared to the increase in performance that they provide. Figure 8 demonstrates how the net efficiency and discharging net work output vary with turbine inlet temperature. TSRC-sCO_2 cycles consistently have lower net efficiencies than RC-sCO_2 cycles which indicates that less energy is generated per unit solar heat input over a complete charge-discharge cycle. However, time-shifting the recompression has potential benefits as the net discharging work (and heat engine efficiency) increase – for a given solar field size a larger quantity of power is dispatched to the grid when it is most valuable. Thus, both the net efficiency and heat engine efficiency should be considered when comparing TSRC-sCO_2 cycles to conventional cycles.

The TSRC-sCO_2 cycle also provides energy storage services to the grid, and the efficacy of this system can be evaluated by comparing the exergetic efficiency to the round-trip efficiency of conventional energy storage systems. The variation in $\eta_{rt,x}$ with turbine inlet temperature is shown in Figure 9, and efficiencies over 70% are reached at turbine inlet temperatures of around 625°C. The TSRC-sCO_2 cycle achieves storage efficiencies that are comparable with the sCO_2 and ideal-gas cycles described earlier. In particular, the TSRC-sCO_2 round-trip efficiency is significantly higher than the ideal-gas cycles at less extreme temperatures (less than 500°C).

TABLE 3. Design point and results for nominal RC-sCO_2 and TSRC-sCO_2 cycles with a 650°C turbine inlet temperature. Work and heat terms are given per unit mass flow rate through the turbine in the discharging phase. CIT: Compressor inlet temperature. TIT: Turbine inlet temperature.

		RC-sCO_2	TSRC-sCO_2 with hot storage	TSRC-sCO_2 with hot and cold storage
Charging cycle				
T_1	°C	-	130.0	130.0
T_2	°C	-	246.4	246.4
T_3	°C	-	40.0	40.0
T_4	°C	-	23.4	23.4
P_1	bar	-	80.0	80.0
β_{chg}	-	-	3.0	3.0
$\dot{W}_{\mathrm{chg}}^{\mathrm{net}}$	$kJ/kg_{dis,\ turb}$	-	26.2	35.9
$\dot{m}/\dot{m}_{\mathrm{dis}}^{\mathrm{turb}}$	-	-	0.35	0.47
Discharging cycle				
CIT	°C	40.0	40.0	35.0
TIT	°C	650.0	650.0	650.0
$\dot{w}_{\mathrm{dis}}^{\mathrm{comp}}$	$kJ/kg_{dis,\ turb}$	61.7	50.6	42.2
$w_{\mathrm{dis}}^{\mathrm{exp}}$	$kJ/kg_{dis,\ turb}$	169.4	169.5	169.5
$\dot{w}_{\mathrm{dis}}^{\mathrm{net}}$	$kJ/kg_{dis,\ turb}$	107.7	118.9	127.2
$\dot{q}_{\mathrm{sol}}$	$kJ/kg_{dis,\ turb}$	221.5	221.1	221.1
η_{HE}	%	48.6	53.8	57.5
$\eta_{rt,x}$	%	-	69.7	70.6
η_{net}	%	48.6	41.9	41.3
$\dot{m}_{\mathrm{dis}}^{\mathrm{recomp.}}/\dot{m}_{\mathrm{dis}}^{\mathrm{turb}}$	-	0.24	-	-

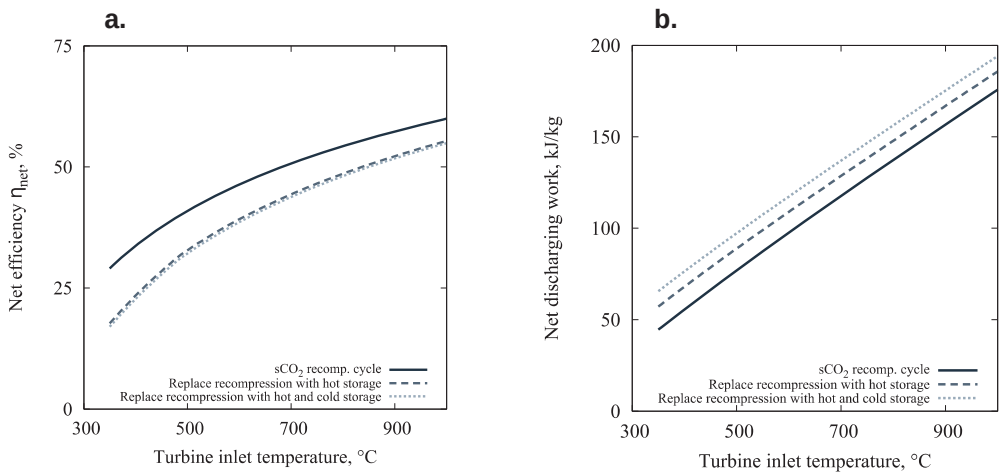

FIGURE 8. Comparison of a sCO_2 recompression cycle with systems that use a heat pump to provide additional heat. Cooling may also be used to reduce compressor inlet temperatures. a) The net efficiency b) The net work output during discharge

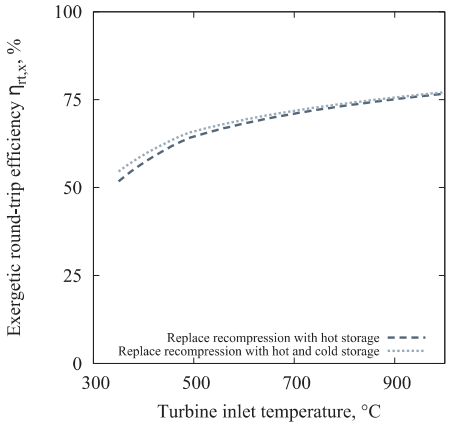

FIGURE 9. Exergetic round-trip efficiency of an TSRC-sCO_2 cycle

CONCLUSIONS

In this article, Pumped Thermal Electricity Storage (PTES) devices which use supercritical carbon dioxide as the working fluid are introduced and compared to PTES cycles based on ideal gases. sCO_2-based cycles are found to have higher work ratios than ideal gas cycles at comparable temperatures, and this leads to potentially higher round-trip efficiencies. The sensitivity of PTES to various loss factors was investigated. PTES cycles use a heat pump during charge and a heat engine during discharge, and each phase involves at least one compression and expansion. These cycles are therefore very susceptible to the compression/expansion efficiency, but it was found that sCO_2 cycles are less sensitive to variations in isentropic efficiency than ideal gas cycles due to the higher work ratio. On the other hand, sCO_2-PTES cycles are more sensitive to irreversibilities due to temperature differences between the power cycle working fluid and storage system because large quantities of heat are transferred per unit work. Supercritical CO_2 exhibits large variations in heat capacity, particularly near the critical point, which may lead to the maximum achievable round-trip efficiency being limited predominantly by heat transfer irreversibilities. These preliminary results will be refined in future work to account for heat capacity variations.

A novel method of integrating PTES cycles with concentrated solar power (CSP) is also described. The sCO_2-recompression cycle has been proposed as the next generation of CSP power cycles, but this cycle requires a second ‘recompression’ at temperatures higher than the main cycle pump. In this article, the recompression is ‘time-shifted’

to occur at periods of low electricity prices and the heat of compression is stored. This heat is deployed instead of the recompression when solar electricity is to be dispatched to the grid. Using a heat pump to create this hot storage also leads to the generation of a cold storage, which may subsequently be used to reduce the heat rejection temperature of the CSP power cycle. It is found that the integrated CSP-PTES cycle produces slightly less electricity per unit solar heat input over a charge-discharge cycle than a stand-alone CSP cycle. However, by storing the recompression heat at a low value time, the integrated system is able to produce 10% more work output than the stand-alone CSP cycle during periods when electricity is most valuable. Using the cold storage to reduce the heat rejection temperature increases the work output by 18%. Thus, a CSP cycle integrated with PTES has greater flexibility than a stand-alone CSP cycle and can potentially also provided electricity storage services to the grid.

ACKNOWLEDGMENTS

This work was authored in part by the National Renewable Energy Laboratory, operated by Alliance for Sustainable Energy, LLC, for the U.S. Department of Energy (DOE) under Contract No. DE-AC36-08GO28308. Funding provided by U.S. Department of Energy Office of Energy Efficiency and Renewable Energy Solar Energy Technologies Office. The views expressed in the article do not necessarily represent the views of the DOE or the U.S. Government. The U.S. Government retains and the publisher, by accepting the article for publication, acknowledges that the U.S. Government retains a nonexclusive, paid-up, irrevocable, worldwide license to publish or reproduce the published form of this work, or allow others to do so, for U.S. Government purposes.

This work is supported in part under the EPSRC funded Generation Integrated Energy Storage project, number EP/P023320/1.

REFERENCES

[1] J.D. McTigue, A.J. White, and C.N. Markides, Appl. Energy **137**, 800–811 (2015). doi:10.1016/j.apenergy.2014.08.039.
[2] R.B. Laughlin, J. Renew. Sustain. Energy **9**, (2017). doi:10.1063/1.4994054.
[3] M. Mercangöz, J. Hemrle, L. Kaufmann, A. Z'Graggen, and C. Ohler, Energy **45**, 407–415 (2012). doi:10.1016/j.energy.2012.03.013.
[4] P. Farrés-Antúnez, H. Xue, and A.J. White, J. Energy Storage **18**, 90–102 (2018). doi:10.1016/j.est.2018.04.016.
[5] T. Desrues, J. Ruer, P. Marty, and J.F. Fourmigué, Appl. Therm. Eng. **30**, 425–432 (2010). doi:10.1016/j.applthermaleng.2009.10.002.
[6] J. Howes, Proc. IEEE **100**, 493–503 (2012). doi:10.1109/JPROC.2011.2174529
[7] S. Freund, "From Powerpoint to Power Plant" in *Int. Work. Carnot Batter.* (2018).
[8] A. White, G. Parks, and C.N. Markides, Appl. Therm. Eng. **53**, 291–298 (2013). doi:10.1016/j.applthermaleng.2012.03.030.
[9] H. Chen, T.N. Cong, W. Yang, C. Tan, Y. Li, and Y. Ding, Prog. Nat. Sci. **19**, 291–312 (2009). doi:10.1016/j.pnsc.2008.07.014.
[10] P. Farrés-Antúnez, *Modelling and Development of Thermo-Mechanical Energy Storage*, PhD Thesis, University of Cambridge. (2018). doi:https://doi.org/10.17863/CAM.38056.
[11] J. McTigue, *Analysis and Optimisation of Thermal Energy Storage*, PhD Thesis, University of Cambridge. (2016). https://doi.org/10.17863/CAM.7084.
[12] W.D. Steinmann, Energy **69**, 543–552 (2014). doi:10.1016/j.energy.2014.03.049.
[13] M. Mehos, C. Turchi, J. Vidal, M. Wagner, Z. Ma, C. Ho, W. Kolb, C. Andraka, and A. Kruizenga, NREL Tech. Report, NREL/TP-5500-67464 (2017).
[14] T. Neises and C. Turchi, Sol. Energy **181**, 27–36 (2019). doi:10.1016/j.solener.2019.01.078.